Preparation, Structure, and Magnetic Properties of Copper(II) Phosphonates. β-$Cu^{II}(CH_3PO_3)$, an Original Three-Dimensional Structure with a Channel-Type Arrangement

Jean Le Bideau,† Christophe Payen,† Pierre Palvadeau,† and Bruno Bujoli*,‡

Laboratoire de Synthèse Organique, URA CNRS 475, and Institut des Matériaux de Nantes, UM CNRS 0110, 2 Rue de la Houssinière, 44072 Nantes Cedex 03, France

Received April 13, 1994[⊗]

Various copper(II) phosphonates are obtained, according to the method of preparation: $Cu(RPO_3)\cdot H_2O$, α-$Cu(RPO_3)$ (R = CH_3, C_2H_5, C_6H_5), β-$Cu(CH_3PO_3)$, and $Cu_3O(CH_3PO_3)_2\cdot 2H_2O$. β-$Cu(CH_3PO_3)$, $a = b = 16.343(6)$ Å, $c = 7.092(4)$ Å, $Z = 18$, $R = 0.021$, and $R_w = 0.025$, is rhombohedral ($R\bar{3}$, No. 148) and has an original channel-type arrangement. $Cu_3O(CH_3PO_3)_2\cdot 2H_2O$ crystallizes in the monoclinic $P2_1/m$ (No. 11) space group with $a = 7.125(4)$ Å, $b = 6.944(4)$ Å, $c = 11.337(7)$ Å, $\beta = 95.33(4)°$, $Z = 2$, $R = 0.055$, and $R_w = 0.061$. The evolution of the anhydrous α-$Cu(RPO_3)$ compounds, in water, in an autoclave at 200 °C, depending on the nature of the R radical, is described. Magnetic susceptibility data for all these copper phosphonates are also reported.

Introduction

In a recent paper, we have reported the synthesis, crystal structure, and magnetic properties of $Fe^{II}(C_2H_5PO_3)\cdot H_2O$ for which a spin-canting phenomenon has been established.[1] Therefore the field of our magnetic measurements has been extended to the other $M^{II}(RPO_3)\cdot H_2O$ lamellar compounds (M = Mn, Co, Ni; R = CH_3, C_2H_5, C_6H_5, n-C_4H_9)[2] that are isostructural to the iron 2+ phosphonate.[3] The case of the copper(II) phosphonates $Cu(RPO_3)\cdot H_2O$ has also been considered from a chemical and structural point of view. Interestingly, the structure of these materials is different from the members of the above family, and a structural rearrangement involving a change in the coordination environment around Cu was postulated for the anhydrous α-$Cu(RPO_3)$ (R = CH_3, C_6H_5, $CH_2C_6H_5$), obtained by thermal treatment of the corresponding hydrates, with an interlayer spacing increase of about 1 Å.[4] This hypothesis of structure evolution occurring during dehydration was later confirmed[5] by the structure determination of α-$Cu(C_2H_5PO_3)$ [$a = 10.7773(3)$ Å, $b = 5.6960(2)$ Å, $c = 7.6273(2)$ Å, $\beta = 94.47(1)°$], prepared by direct synthesis from copper nitrate and ethylphosphonic acid. In the present paper, we report now all the results of our attempts concerning the direct synthesis of α-$Cu(RPO_3)$ (R = CH_3, C_2H_5, C_6H_5). Thus, two new copper phosphonates A, β-$Cu(CH_3PO_3)$ (with magnetic susceptibility, IR, and X-ray data strongly different from that of α-$Cu(CH_3PO_3)$ issued from thermal treatment), and B, $Cu_3O(CH_3PO_3)_2\cdot 2H_2O$, were produced and their structures have been determined. Then, some relationships between the structure and the magnetic susceptibility data are discussed for the $Cu(RPO_3)\cdot H_2O$ and α-$Cu(RPO_3)$ series as well as for compounds A and B.

Experimental Section

Preparation of Copper Phosphonates. Chemicals used were of reagent grade quality and were obtained from Aldrich without further purification. The different ways of preparation of the copper phosphonates are summarized in Scheme 1. The samples of $Cu(RPO_3)\cdot H_2O$ (R = CH_3, C_2H_5, C_6H_5) and crystalline α-$Cu(C_2H_5PO_3)$ were prepared as previously described.[5] The poorly crystallized anhydrous compounds α-$Cu(RPO_3)$ (R = CH_3, C_2H_5, C_6H_5) were obtained from the corresponding hydrates after thermal treatment in air at 200 °C for 3 h. β-$Cu(CH_3PO_3)$ and $Cu_3O(CH_3PO_3)_2\cdot 2H_2O$ were prepared by placing 0.75 mmol of α-$Cu(CH_3PO_3)$ (see above) with water in the Teflon cell (20 mL capacity) of an autoclave that was then sealed and placed in a drying oven at 200 °C for 15 days. The product obtained was filtered off with suction, washed with water, and dried under vacuum. In fact, a mixture of pale green needles (around 95%) of β-$Cu(CH_3PO_3)$ and blue plates (around 5%) of $Cu_3O(CH_3PO_3)_2\cdot 2H_2O$ was produced, and the two compounds were separated for their characterization and X-ray structure determination. The composition of the two compounds was also confirmed by chemical analyses of hydrogen and carbon. β-$Cu(CH_3PO_3)$: % H (calcd, 1.90; found, 1.85); % C (calcd, 7.62; found, 7.69). In the case of $Cu_3O(CH_3PO_3)_2\cdot 2H_2O$ [% H (calcd, 2.32, found, 2.31); % C (calcd, 5.57; found, 5.49)], the loss of water (190 °C) was concomitant with P–C bond scission and no indication could be deduced from TGA measurements.

Crystallographic Study. All measurements for compounds A and B were made on an Enraf-Nonius CAD-4 diffractometer with graphite-monochromated Mo Kα radiation. Cell constants and an orientation matrix for data collection were obtained from least-squares refinements, with use of the setting angles of 25 randomly oriented reflections in the range $10° \le 2\theta \le 35°$. The data were collected out to 60° in 2θ using the $\omega-2\theta$ scan technique (compound A, $h = -25$ to 25, $k = 0$ to 25, $l = 0$ to 11; compound B, $h = -11$ to 11, $k = 0$ to 11, $l = 0$ to 18). To check on crystal and instrument stability, three representative reflections were measured every 60 min and no decay was observed. Empirical absorption corrections based on the ψ scan measurements were applied, and the data were corrected for Lorentz and polarization effects. For the data reduction, structure solution, and refinement, the MOLEN program (1990 version), written by Kay Fair, was used on a microVAX 3900 computer. The atomic scattering factors were taken

† UM CNRS 0110.
‡ URA CNRS 475.
⊗ Abstract published in *Advance ACS Abstracts,* September 1, 1994.

(1) Bujoli, B.; Pena, O.; Palvadeau, P.; Le Bideau, J.; Payen, C.; Rouxel, J. *Chem. Mater.* **1993**, *5*, 583.
(2) Le Bideau, J. Ph.D. Thesis, Nantes, 1994.
(3) Cunningham, D.; Hennely, P. J. D.; Deeney, T. *Inorg. Chim. Acta* **1979**, *37*, 95. Cao, G.; Lee, H.; Lynch, V. M.; Mallouk, T. E. *Inorg. Chem.* **1988**, *27*, 2781. Martin, K. J.; Squattrito, P. J.; Clearfield, A. *Inorg. Chim. Acta* **1989**, *155*, 7.
(4) Zhang, Y.; Clearfield, A. *Inorg. Chem.* **1992**, *31*, 2821. Zhang, Y.; Scott, K. J.; Clearfield, A. *Chem. Mater.* **1993**, *5*, 495.
(5) Le Bideau, J.; Bujoli, B.; Jouanneaux, A.; Payen, C.; Palvadeau, P.; Rouxel, J. *Inorg. Chem.* **1993**, *32*, 4617.

0020-1669/94/1333-4885$04.50/0

Scheme 1

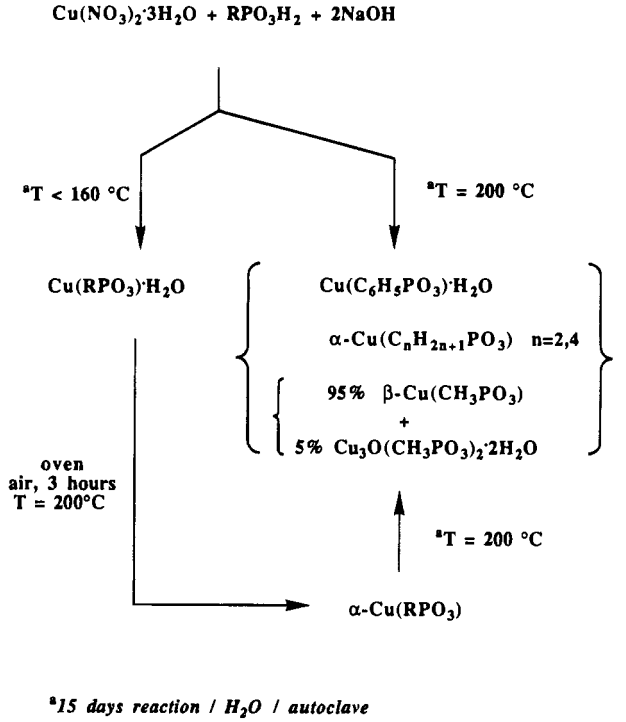

from Cromer and Waber,[6] and anomalous dispersion corrections were taken from Cromer and Ibers.[7]

β-Cu(CH_3PO_3). A green needle having approximate dimensions 0.06 × 0.06 × 0.6 mm^3 was mounted on a glass fiber. The structure was determined in the $R\bar{3}$ space group (No. 148). The positions of the copper and phosphorus atoms were determined from a three-dimensional Patterson map, with the oxygen and the carbon atoms being found from successive difference Fourier maps. The non-hydrogen atoms were refined anisotropically, and all the hydrogen atoms were located from ΔF maps and refined with fixed thermal parameters. A total of 3116 reflections were measured, of which 764 were unique with the condition $I \geq 5\sigma(I)$ (65 variables). The final cycle of full-matrix least-squares refinement converged (largest parameter shift was 0.03 times its esd) with unweighted and weighted agreement factors of $R = 0.021$ and $R_w = 0.025$.

$Cu_3O(CH_3PO_3)_2 \cdot 2H_2O$. The data were collected on a blue platelet of approximate dimensions 0.04 × 0.4 × 0.16 mm^3. On the basis of the systematic absences ($0k0$, $k = 2n + 1$) and the successful refinement of the structure, the space group was found to be $P2_1/m$ (No. 11). The positions of the copper and phosphorus atoms were determined from a three-dimensional Patterson map, with the oxygen and the carbon atoms being found from successive ΔF maps. The non-hydrogen atoms were refined anisotropically. On the final difference Fourier map, some peaks were located close to the positions of O(5) and O(7) and could be assumed to correspond to hydrogen atoms; however, attempts to refine these positions with B thermal parameters fixed at 4.0 were not successful, leading to inconsistent values for O−H bond lengths. Of the 4021 reflections which were collected, 1075 were unique and observed with $I \geq 3\sigma(I)$ (89 variables). The final cycle of full-matrix least-squares refinement converged with unweighted and weighted agreement factors of $R = 0.055$ and $R_w = 0.061$. Crystallographic data for β-Cu(CH_3PO_3) and $Cu_3O(CH_3PO_3)_2 \cdot 2H_2O$ are listed in Table 1.

Magnetic Data. Magnetic susceptibility measurements were carried out on a MPMS5 Quantum Design SQUID magnetometer using powdered samples which were initially zero-field cooled down to 5 K and then warmed up to 300 K in a static applied field of 5 kOe. Data were first corrected for the sample holder effects and then for the diamagnetism contribution estimated from Pascal's constants. Magnetic moments were calculated from the formula $\mu_{eff}/\mu_B = 2.828\ (\chi_M T)^{1/2}$, where χ_M is the susceptibility expressed in emu/mol of Cu.

(6) Cromer, D. T.; Waber, J. T. *International Tables for X-ray Crystallography*; Kynoch Press: Birmingham, England, 1974; Vol. IV, Table 2.2B.

(7) Cromer, D. T.; Ibers, J. A. *International Tables for X-ray Crystallography*; Kynoch Press: Birmingham, England, 1974; Vol. IV, Table 2.3.1.

Table 1. Crystallographic Data for β-Cu(CH_3PO_3) and $Cu_3O(CH_3PO_3)_2 \cdot 2H_2O$

	β-Cu(CH_3PO_3)	$Cu_3O(CH_3PO_3)_2 \cdot 2H_2O$
empirical formula	$CuPO_3CH_3$	$Cu_3P_2O_9C_2H_{10}$
fw	157.55	430.66
a, Å	16.343(6)	7.125(4)
b, Å	16.343(6)	6.944(4)
c, Å	7.092(4)	11.337(7)
α, deg	90	
β, deg	90	95.33(4)
γ, deg	120	
V, Å^3	1640(1)	562.5(8)
Z	18	2
space group	$R\bar{3}$ (No. 148)	$P2_1/m$ (No. 11)
$R(F_o)^a$	0.021	0.055
$R_w(F_o)^b$	0.025	0.061

[a] $R(F_o) = \sum||F_o| - |F_c||/\sum|F_o|$. [b] $R_w(F_o) = [\sum w(|F_o| - |F_c|)^2/\sum w(F_o^2)]^{1/2}$; $w = 4F_o^2/(\sigma(F_o^2))^2$.

Table 2. Positional and Thermal Parameters for the Atoms of β-Cu(CH_3PO_3)

atom	x	y	z	B_{eq},[a] Å^2
Cu	0.06135(2)	0.40288(2)	0.37830(6)	0.714(6)
P	0.16831(5)	0.89469(5)	0.0924(1)	0.65(1)
O(1)	0.0888(2)	0.5007(2)	0.5553(3)	0.98(4)
O(2)	0.4529(1)	0.0141(2)	0.2118(3)	0.84(4)
O(3)	0.3405(2)	0.2700(2)	0.8464(3)	0.94(4)
C	0.4961(2)	0.2159(2)	0.5711(5)	1.27(6)
H(1)	0.133(4)	0.059(4)	0.801(9)	4.0
H(2)	0.181(4)	0.660(4)	0.433(9)	4.0
H(3)	0.224(4)	0.743(4)	0.310(8)	4.0

[a] The copper, phosphorus, oxygen, and carbon atoms were refined anisotropically and their B values are given in the form of the equivalent displacement parameter defined as $B_{eq} = {}^4/_3\sum_i\sum_j\beta_{ij}A_iA_j$.

Table 3. Bond Lengths (Å) and Angles (deg) for the Non-Hydrogen Atoms of β-Cu(CH_3PO_3)

Cu−O(1)	1.902(2)	P−O(1)	1.515(2)
Cu−O(2)	1.997(3)	P−O(2)	1.556(2)
Cu−O(2)	1.995(2)	P−O(3)	1.526(2)
Cu−O(3)	1.937(2)	P−C	1.787(3)
Cu−O(3)	2.307(3)		
O(1)−Cu−O(2)	91.4(1)	O(2)−Cu−O(3)	83.6(1)
O(1)−Cu−O(2)	93.7(1)	O(3)−Cu−O(3)	90.9(1)
O(1)−Cu−O(3)	109.5(1)	O(1)−P−O(2)	110.9(1)
O(1)−Cu−O(3)	159.6(1)	O(1)−P−O(3)	110.1(1)
O(2)−Cu−O(2)	171.3(1)	O(1)−P−C	109.1(2)
O(2)−Cu−O(3)	74.7(1)	O(2)−P−O(3)	111.3(2)
O(2)−Cu−O(3)	94.0(1)	O(2)−P−C	105.5(2)
O(2)−Cu−O(3)	96.9(1)	O(3)−P−C	109.8(1)

Results

Structure of β-Cu(CH_3PO_3). Positional and thermal parameters of the atoms in this structure are given in Table 2, and selected bond distances and angles are listed in Table 3. Each Cu atom has a distorted tetragonal pyramidal coordination, and the four coplanar oxygen atoms have bond distances in the range 1.902(2)−1.997(3) Å. The fifth oxygen is nearly perpendicular to the plane and has a bond length of 2.307(3) Å. The three oxygens of the phosphonate groups are all bonded to Cu atoms. Two of them bridge copper atoms which are 3.0102(5) Å apart. This structure is three-dimensional and consists of infinite zigzag chains of copper running parallel to the c-axis (Figure 1). Each copper atom is connected to two

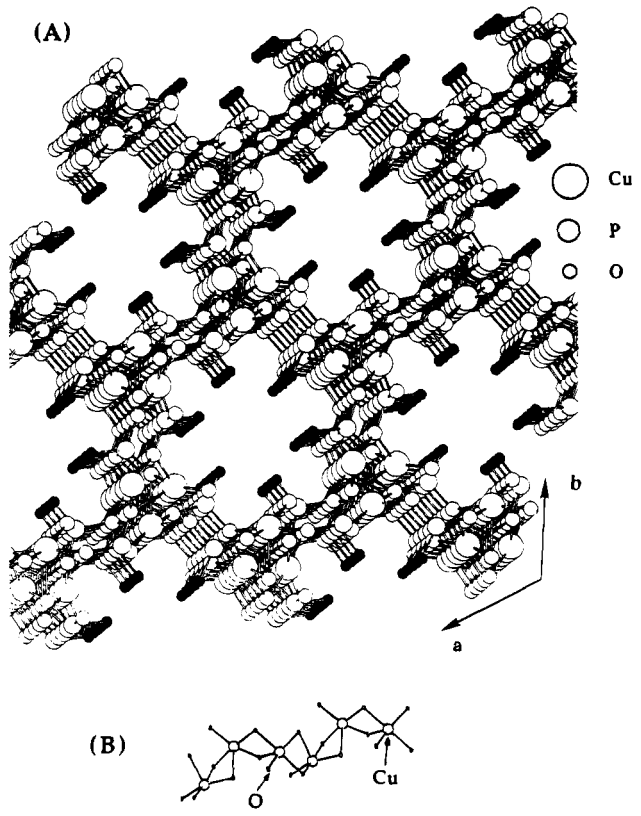

Figure 1. (A) Perspective representation of β-$Cu(CH_3PO_3)$ viewed down the *c*-axis, illustrating the tubular structure. The carbon atoms are depicted in black. (B) Visualization of a copper chain along the *c*-axis.

Table 4. Positional and Thermal Parameters for the Atoms of $Cu_3O(CH_3PO_3)_2{\cdot}2H_2O$

atom	*x*	*y*	*z*	B_{eq},[a] Å^2
Cu(1)	0.0484(2)	0.4945(2)	0.3717(1)	1.24(2)
Cu(2)	0.6869(3)	0.25	0.4322(2)	1.38(3)
P(1)	0.3353(5)	0.25	0.2346(4)	1.33(7)
P(2)	0.3026(5)	0.25	0.5890(4)	1.19(7)
O(1)	0.1812(9)	0.070(1)	0.5543(7)	1.5(1)
O(2)	0.541(2)	0.25	0.281(1)	2.2(2)
O(3)	0.236(1)	0.066(1)	0.2686(7)	1.8(1)
O(4)	0.477(2)	0.25	0.526(1)	1.8(2)
O(5)	0.839(1)	0.25	0.598(1)	1.4(2)
O(6)	0.918(1)	0.25	0.344(1)	1.3(2)
O(7)	0.861(3)	0.25	0.890(2)	4.8(4)
C(1)	0.331(3)	0.25	0.076(2)	2.4(4)
C(2)	0.360(3)	0.25	0.746(2)	2.0(3)

[a] See footnote *a* of Table 2.

adjacent copper atoms by oxygen bridges forming four-membered rings (Cu−O(2)−Cu−O(3)) that are distorted parallelogram-shaped with two Cu−O distances close to 2 (1.997(2) Å and 1.995(2) Å) and one short and one long Cu−O bond (1.937(2) and 2.307(3) Å). These chains are linked together in the *a,b* plane by O−P−O bridges, forming hexagonal tunnels parallel to the *c*-axis. The methyl groups are extending in the space of these tunnels.

Structure of $Cu_3O(CH_3PO_3)_2{\cdot}2H_2O$. Positional and thermal parameters of the atoms in this structure are given in Table 4, and selected bond distances and angles are listed in Table 5. The structure is layered. Figure 2 shows the coordination environment of the two types of Cu atoms and the numbering scheme used in the tables. One of them, Cu(1), has a distorted (4 + 1) tetragonal pyramidal coordination. The four coplanar oxygen atoms (two phosphonate oxygens, $O(1)^a$, $O(3)^b$, one "oxide type" oxygen, $O(6)^d$, and one water oxygen, $O(5)^c$) have

Table 5. Bond Lengths (Å) and Angles (deg) for the Non-Hydrogen Atoms of $Cu_3O(CH_3PO_3)_2{\cdot}2H_2O$

$Cu(1)-O(1)^a$	1.978(8)	Cu(2)−O(6)	2.00(1)
$Cu(1)-O(1)^b$	2.240(8)	P(1)−O(2)	1.51(1)
$Cu(1)-O(3)^b$	1.904(8)	P(1)−O(3)	1.535(9)
$Cu(1)-O(5)^c$	1.976(5)	$P(1)-O(3)^b$	1.535(9)
$Cu(1)-O(6)^d$	1.956(5)	P(1)−C(1)	1.79(2)
$Cu(2)-O(1)^e$	2.426(8)	P(2)−O(1)	1.558(8)
$Cu(2)-O(1)^c$	2.426(8)	$P(2)-O(1)^b$	1.558(8)
Cu(2)−O(2)	1.92(1)	P(2)−O(4)	1.49(1)
Cu(2)−O(4)	1.91(1)	P(2)−C(2)	1.79(2)
Cu(2)−O(5)	2.08(1)		
$O(1)^a-Cu(1)-O(1)^b$	87.5(3)	O(2)−Cu(2)−O(4)	96.2(5)
$O(1)^a-Cu(1)-O(3)^b$	167.3(3)	O(2)−Cu(2)−O(5)	178.6(5)
$O(1)^a-Cu(1)-O(5)^c$	91.4(4)	O(2)−Cu(2)−O(6)	87.6(5)
$O(1)^a-Cu(1)-O(6)^d$	84.4(4)	O(4)−Cu(2)−O(5)	82.4(5)
$O(1)^b-Cu(1)-O(3)^b$	105.2(3)	O(4)−Cu(2)−O(6)	176.2(5)
$O(1)^b-Cu(1)-O(5)^c$	83.8(4)	O(5)−Cu(2)−O(6)	93.8(4)
$O(1)^b-Cu(1)-O(6)^d$	97.1(4)	O(2)−P(1)−O(3)	111.6(4)
$O(3)^b-Cu(1)-O(5)^c$	90.6(4)	$O(2)-P(1)-O(3)^b$	111.6(4)
$O(3)^b-Cu(1)-O(6)^d$	93.3(4)	O(2)−P(1)−C(1)	105.9(9)
$O(5)^c-Cu(1)-O(6)^d$	175.6(4)	$O(3)-P(1)-O(3)^b$	114.1(5)
$O(1)^e-Cu(2)-O(1)^c$	134.5(2)	O(3)−P(1)−C(1)	106.6(5)
$O(1)^e-Cu(2)-O(2)$	103.3(2)	$O(3)^b-P(1)-C(1)$	106.6(5)
$O(1)^e-Cu(2)-O(4)$	106.5(2)	$O(1)-P(2)-O(1)^b$	107.9(4)
$O(1)^e-Cu(2)-O(5)$	77.1(2)	O(1)−P(2)−O(4)	110.2(4)
$O(1)^e-Cu(2)-O(6)$	72.5(2)	O(1)−P(2)−C(2)	108.8(5)
$O(1)^c-Cu(2)-O(2)$	103.3(2)	$O(1)^b-P(2)-O(4)$	110.2(4)
$O(1)^c-Cu(2)-O(4)$	106.5(2)	$O(1)^b-P(2)-C(2)$	108.8(5)
$O(1)^c-Cu(2)-O(5)$	77.1(2)	O(4)−P(2)−C(2)	110.9(8)
$O(1)^c-Cu(2)-O(6)$	72.5(2)		

[a] Atom related by the following transformations: $-x$, $^1/_2 + y$, $1 - z$;[b] x, $^1/_2 - y$, z;[c] $1 - x$, $^1/_2 + y$, $1 - z$;[d] $x - 1$, y, z;[e] $1 - x$, $-y$, $1 - z$.

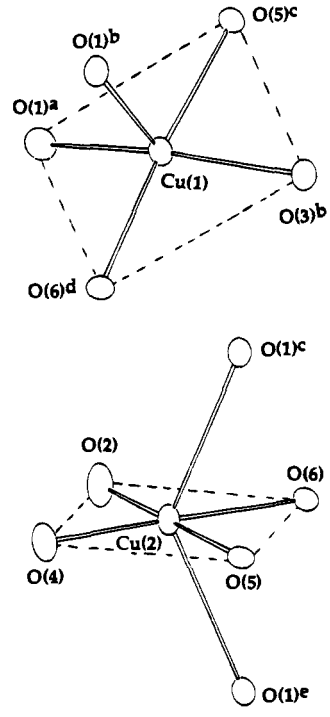

Figure 2. Schematic representation of the coordination about the two types of copper atoms in $Cu_3O(CH_3PO_3)_2{\cdot}2H_2O$ and the numbering scheme used in the tables.

bond distances in the range 1.908(6)−1.976(3) Å. The fifth oxygen $O(1)^b$ is nearly perpendicular to the plane with a bond length of 2.244(6) Å. The second copper atom Cu(2) has a distorted (4 + 2) octahedral coordination. The four coplanar oxygen atoms (two phosphonate oxygens, O(2) and O(4), and again the O(5) and O(6) oxygens) have bond distances in the range 1.914(9)−2.078(9) Å. The two last oxygens $O(1)^c$ and

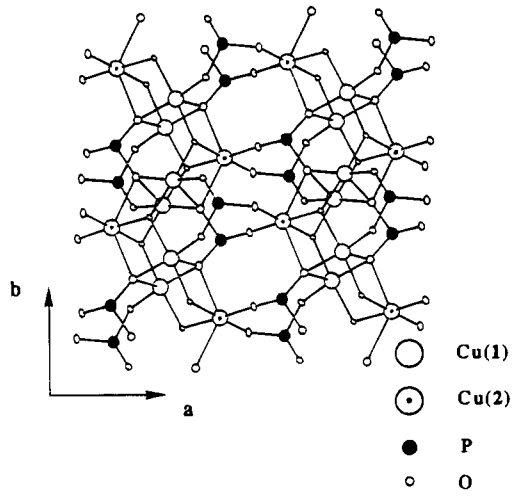

Figure 3. Schematic representation of a $Cu_3O(CH_3PO_3)_2{\cdot}2H_2O$ layer as seen perpendicular to the *c*-axis. The carbon atoms and the water molecule O(7) have been omitted for clarity.

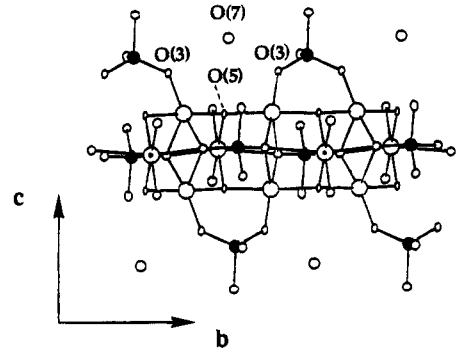

Figure 4. Schematic representation of a $Cu_3O(CH_3PO_3)_2{\cdot}2H_2O$ layer as seen perpendicular to the *a*-axis.

O(1)[e] have rather long bond lengths of 2.423(6) Å, situated above and below the mean plane of the four equatorial bonds and inclined at an angle around 75° with this plane. The oxygens of the phosphonate groups are all bonded to Cu atoms (Figure 3). For atom P(1), each of the three oxygens are bonded to only one copper atom (2 Cu(1) and 1 Cu(2)) while, for atom P(2), there are two bridging oxygens O(1) and O(1)[b]. Each of them bridges two different pairs of Cu(1) atoms which are 3.052-(2) Å apart. These same two copper atoms are bridged by a second O(1) atom from another phosphonate group, forming four-membered parallelogram-shaped ring. The third P(2) phosphonate oxygen O(4) is coordinated to a Cu(2) atom. The layer then consists of four-membered rectangular Cu(1)−O(1)−Cu(1)−O(1) rings running in the *b*-axis direction. On one side these rings are linked together by two O−P−O bridges (O(1)−P(2)−O(1) and O(3)−P(1)−O(3)). On the other side the connection is ensured by two bridging oxygens (O(5) and O(6)) and one O(1)−Cu(2)−O(1) bridge (d(Cu(1)−Cu(2)) = 3.129-(2) and 3.303(2) Å). Thus, the copper atoms form chains along the *b*-axis, via a zigzag Cu−O−Cu linking. These chains are linked together in the *a*-axis direction by O(2)−P(1)−O(3) and O(1)−P(2)−O(4) bridges. The layers are situated perpendicular to the *c*-axis with an interlayer spacing equal to *c*, as shown in Figure 4. The methyl groups are pointing toward the interlamellar space, above and below the CuO_3P inorganic layers, making Van der Waals contacts between these layers. The water molecule O(7) is present in the interlayer space, close to O(3) (2.89(1) Å) and to the other water molecule O(5) (3.30(2) Å) (see Figure 4), with probably hydrogen-bond interactions between these three oxygens.

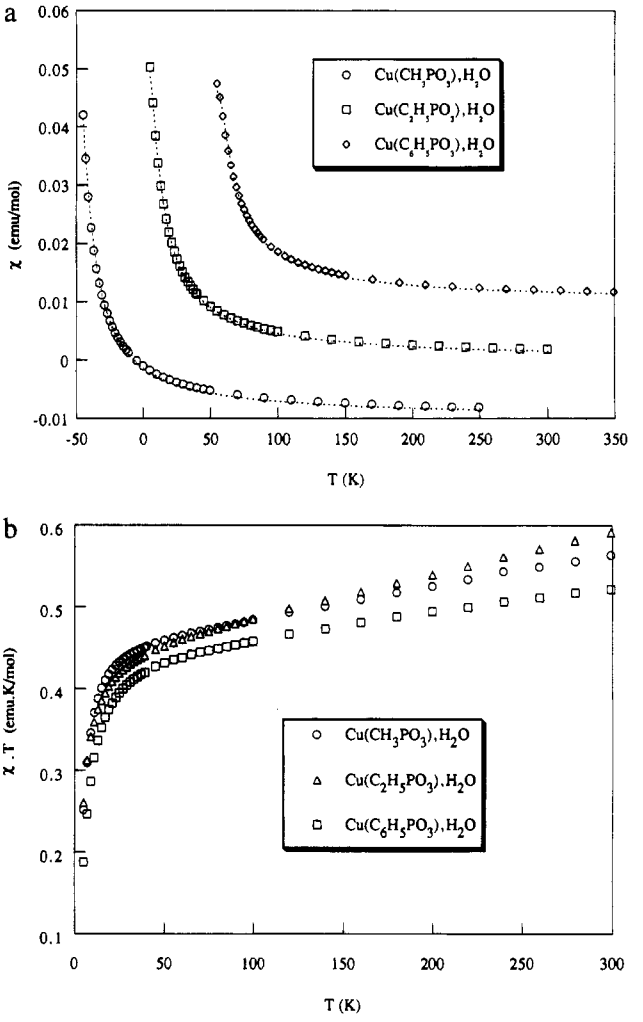

Figure 5. Thermal evolution of (a) the molar susceptibility and (b) the $\chi_M T$ product for the $Cu(RPO_3){\cdot}H_2O$ compounds (R = CH_3, C_2H_5, C_6H_5). In (a) susceptibility and temperature scales are shown for R = C_2H_5; values for other R groups are offset by ±50 K/±0.01 emu/mol. The dashed lines in (a) are for the best fit, as explained in the text.

However, it should be noted that O(5) and O(6) have similar environments, bond lengths, and thermal parameters, thus suggesting another possibility for the formulation of compound B: $Cu_3(OH)_2(CH_3PO_3)_2{\cdot}H_2O$, in which O(5) and O(6) would be "hydroxide" oxygens. Unfortunately, TGA data cannot help to distinguish between the two formulations because the loss of water (190 °C) is concomitant with the P−C bond scission. Moreover, attempts to refine possible hydrogen positions (deduced from a ΔF map) near O(5) and O(7), with B thermal parameters fixed at 4.0, were not successful and led to inconsistent values for O−H bond lengths. Consequently, the possibility of having the $Cu_3(OH)_2(CH_3PO_3)_2{\cdot}H_2O$ formulation for compound B cannot be excluded.

Magnetic Properties. Magnetic behaviors of the $Cu(RPO_3){\cdot}H_2O$, α-$Cu(RPO_3)$ (R = CH_3, C_2H_5, C_6H_5), β-$Cu(CH_3PO_3)$, and $Cu_3O(CH_3PO_3)_2{\cdot}2H_2O$ compounds are depicted in Figures 5−8. The χ_M and $\chi_M T$ product vs T curves for the $Cu(RPO_3){\cdot}H_2O$ show that these compounds have very similar behavior (Figure 5). The room-temperature magnetic moments range from 2.0 to 2.2 μ_B/Cu. At low temperature (T < 20 K) the $\chi_M T$ product drastically decreases revealing weak antiferromagnetic interactions between the copper(II) ions (Figure 5b). The room-temperature magnetic moments of the anhydrous α-$Cu(RPO_3)$ compounds range from 1.9 to 2.2 μ_B/Cu. With decreasing temperature the susceptibilities pass through broad

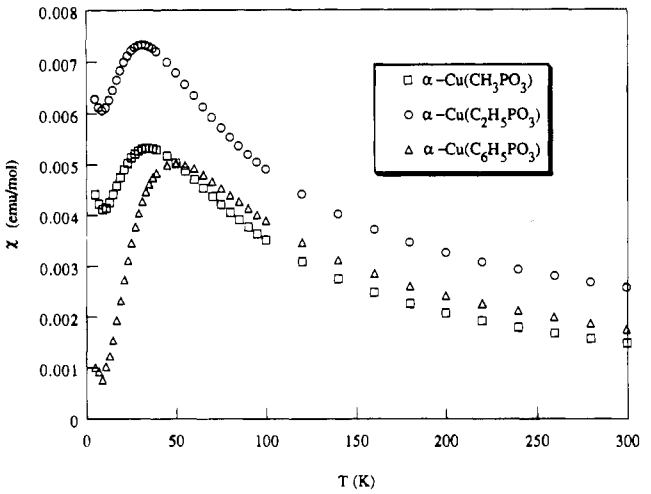

Figure 6. Thermal evolution of the molar susceptibilities for the α-Cu^{II}-(RPO_3) compounds (R = CH_3, C_2H_5, C_6H_5).

maxima at about 35 K for R = CH_3 and C_2H_5 and 50 K for R = C_6H_5 (Figure 6). Such behaviors are characteristic of low-dimensional antiferromagnets. The increase of the susceptibilities observed below about 10 K are probably due to uncoupled paramagnetic species. At room temperature a magnetic moment of 2.1 μ_B/Cu is observed for β-Cu(CH_3PO_3). The susceptibility curve also exhibits a maximum located at 15 K (Figure 7). The room-temperature magnetic moment for $Cu_3O(CH_3PO_3)_2 \cdot 2H_2O$ is equal to 2.1 μ_B/Cu. The $\chi_M T$ product then continuously decreases till 70 K where it seems to reach a plateau (Figure 8), perhaps indicating a lowering of the effective moment of the Cu(II) ions in this region. At very low temperature (T < 10 K) the $\chi_M T$ product drops to zero showing that the compound possesses a $S = 0$ antiferromagnetic ground state (Figure 8).

Discussion

According to the crystal structure analysis of the Cu($RPO_3 \cdot H_2O$ (R = CH_3, C_6H_5) lamellar compounds, two adjacent copper atoms are bridged by oxygen atoms so four-membered parallelogram-shaped Cu−O−Cu−O rings are formed within a slab.[4] Two next-nearest neighboring copper atoms are linked by O−P−O bridges. Neglecting this latter type of path, the presence of magnetically coupled Cu−Cu dimers could be anticipated. Effectively, the susceptibility data could be fitted using the simple Bleaney−Bowers dinuclear law for a Heisenberg−Hamiltonian H = $-2JS_1S_2$:

$$\chi = \frac{Ng^2\mu_B^2}{kT}\frac{1}{3 + \exp(-2J/kT)}$$

where $|2J|$ is the singlet−triplet energy gap and N, g, μ_B, k, and T have their usual meaning. The best fit results are shown in Figure 5a and given in Table 6. The exchange coupling constant for R = C_6H_5 is slightly higher than for R = CH_3 and C_2H_5. Taking into account interdimer interactions by means of a molecular field term did not improve the fits. The antiferromagnetic values of J are consistent with the observed decrease of the $\chi_M T$ products at low temperature (see Table 6 and Figure 5b). These interactions are however very small so that no maximum is detected in the thermal variations of the susceptibilities down to the lowest temperature we proceeded (5 K).

Magnetic superexchange pathways between copper atoms in a slab of the α-Cu($C_2H_5PO_3$) structure are much more numerous than for its hydrated counterparts.[5] These paths form a nonsimple two-dimensional network for which no high-temperature series expansions have been performed. Anyhow, the presence of broad maxima in the susceptibility curves (Figure 6) of the three compounds (R = CH_3, C_2H_5, C_6H_5) clearly show that antiferromagnetic interactions exist within the slabs. The differences in observed behaviors between the three compounds could be due to only very small changes of the environment about the copper atoms (see Figure 6). In particular, a special arrangement of the phenyl groups that would tend to minimize the repulsion between the π−π electronic densities could in turn induce additional distortions of the copper coordination units.

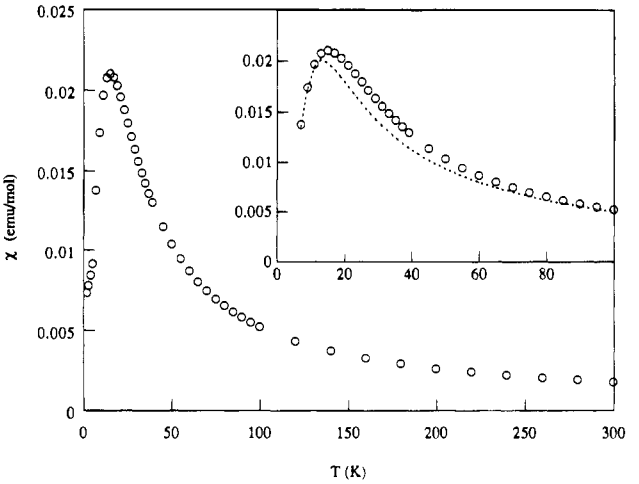

Figure 7. Thermal evolution of the molar susceptibility for β-Cu^{II}(CH_3PO_3). The dashed line in the insert is for the best fit, as explained in the text.

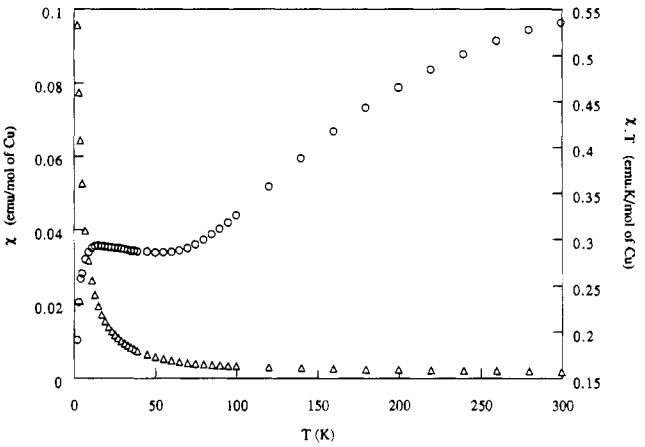

Figure 8. Thermal evolution of the susceptibility/mol of Cu and the $\chi_M T$ product for $Cu_3O(CH_3PO_3)_2 \cdot 2H_2O$.

Table 6. Best Fitted Values of J and g for the $Cu^{II}(RPO_3) \cdot H_2O$ Compounds

	compound		
	Cu(CH_3PO_3)·H_2O	Cu($C_2H_5PO_3$)·H_2O	Cu($C_6H_5PO_3$)·H_2O
J/k (K)	−3.45(5)	−3.78(4)	−4.69(5)
g	2.19(1)	2.23(1)	2.15(1)

Considering the above described chain structure of β-Cu(CH_3PO_3), we tried to reproduce the susceptibility of this compound using various existing calculations for $S = 1/2$ magnetic chains.[8] The best fit was obtained for the relation proposed by Hatfield[9] for an antiferromagnetic alternating one-

(8) Hatfield, W. E.; Estes, W. E.; Marsh, W. E.; Pickens, M. W.; Haar, L. W.; Weller, R. R. In *Extended Linear Chain Compounds;* Miller J. S., Ed.; Plenum Press: New York, 1983; Vol. 3, p 43.

dimensionnal model described by the following isotropic Hamiltonian:

$$H = -2J\sum_i [S_iS_{i-1} + \alpha S_iS_{i+1}]$$

where J is the exchange coupling constant and α the alternation parameter. The susceptibility is expressed[9] as follows:

$$\chi = \frac{Ng^2\mu_B{}^2}{kT}\frac{A + Bx + Cx^2}{1 + Dx + Ex^2 + Fx^3}$$

where $x = |J|/kT$. For $0 < \alpha < 0.4$, the $A-F$ parameters are given by[9]

$$A = 0.25$$

$$B = -0.12587 + 0.22752\alpha$$

$$C = 0.019111 - 0.13307\alpha + 0.509\alpha^2 - 1.3167\alpha^3 + 1.0081\alpha^4$$

$$D = 0.10772 + 1.4192\alpha$$

$$E = -0.0028521 - 0.42346\alpha + 2.1953\alpha^2 - 0.82412\alpha^3$$

$$F = 0.37754 - 0.067022\alpha + 0.59805\alpha^2 - 2.1678\alpha^3 + 15.838\alpha^4$$

The best fit result was obtained for $J/k = -10(2)$ K and $\alpha = 0.20(1)$ with $g = 2.4$. As shown in Figure 7, this fit is however not entirely satisfactory.

The direct synthesis of crystalline α-$Cu(RPO_3)$ was possible for the ethyl group but failed in the case of the methyl and phenyl groups. When R = C_6H_5, the hydrated form was produced. When R = CH_3, two materials were obtained; the major portion was A, β-$Cu(CH_3PO_3)$, with traces of B, $Cu_3O(CH_3PO_3)_2{\cdot}2H_2O$ (Scheme 1). These results are likely a consequence of the stability of the α-$Cu(RPO_3)$ form in the working conditions, because when α-$Cu(RPO_3)$ samples were placed with water in an autoclave at 200 °C for 2 weeks, no modification was observed in the case of the ethyl group while the hydrated form was obtained in the case of the phenyl group (reversibility). When R = CH_3, the two new copper methylphosphonates A and B were isolated again, in the same respective amounts. In the layer arrangement of the three α-$Cu(RPO_3)$ compounds (R = CH_3, C_2H_5, C_6H_5), a relatively rare copper environment (trigonal bipyramidal) is observed, which could probably explain the chemical behavior described in Scheme 1. In our experimental conditions, we could suppose that the copper atoms tend to adopt a more favorable (4 + 1) square pyramidal coordination. In the case of the flat phenyl group, the copper atoms are likely accessible to water molecules, in order to give back the copper phenylphosphonate monohydrate, with a (4 + 1) coordination for copper. This phenomenon does not occur for the two other substituents. In the case of the methyl group, a structure transition from the two-dimensional α-$Cu(CH_3PO_3)$ to the three-dimensional β-$Cu(CH_3PO_3)$ network takes place, and again the coordination around copper is (4 + 1). The presence of 5% of $Cu_3O(CH_3PO_3)_2{\cdot}2H_2O$ is perhaps a consequence of a slight degradation of $Cu(CH_3PO_3)$ in the experimental conditions.

It is worth noting the originality of the β-$Cu(CH_3PO_3)$ compound. To our knowledge, no example of three-dimensional structure has been reported in the literature for phosphonates, which are usually layered, except of course when the phosphonic acid used bears a functional group (such as COOH or NH_2[10]) that is able to coordinate to metal centers. This structure is very close to that of a zinc phosphite[11] $Zn(HPO_3H)_2{\cdot}{}^1/_3H_2O$, with a similar channel-type arrangement in which zinc has an octahedral environment and the H and OH groups point in the space of the hexagonal tunnels. In β-$Cu(CH_3PO_3)$, the hexagonal tunnels allow the structure to accommodate the bulkiness of the methyl groups. The dimension of these tunnels (5.97 Å between two opposite methyl carbons, not including the hydrogen atoms) are too small to get an analog in the case of the ethyl group, and that is probably the reason why no transformation of α-$Cu(C_2H_5PO_3)$ is observed. Consequently, we could then expect a similar chemical behavior for the copper ethyl- and *n*-butylphosphonates. Therefore, at the end of this study, complementary experiments were performed using *n*-butylphosphonic acid. As in the case of the ethyl group, α-Cu-(*n*-$C_4H_9PO_3$) [a = 15.32(1) Å, b = 5.69(1) Å, c = 7.60(1) Å, β = 95.14(3)°] was effectively stable in water (autoclave at 200 °C) and was also directly prepared from copper nitrate and *n*-butylphosphonic acid (see Scheme 1).

Supplementary Material Available: Tables giving a full presentation of the crystal data and anisotropic thermal parameters for nonhydrogen atoms (3 pages). Ordering information is given on any current masthead page. A tabulation of observed and calculated structure factors for the two structures is available upon request from B.B. for up to 1 year from the date of publication.

(9) Hatfield, W. E. *J. Appl. Phys.* **1981**, *52*, 1985.

(10) Cao, G.; Rabenberg, L. K.; Nunn, C. M.; Mallouk, T. E. *Chem. Mater.* **1991**, *3*, 149. Drumel, S.; Janvier, P.; Barboux, P.; Bujoli-Doeuff, M.; Bujoli, B. *Inorg. Chem.*, submitted for publication.

(11) Ortiz-Avila, C. Y.; Squattrito, P. J.; Shieh, M.; Clearfield, A. *Inorg. Chem.* **1989**, *28*, 2608. Durand, J.; Cot, L.; Sghyar, M.; Rafiq, M. *Acta Crystallogr.* **1992**, *C48*, 1171.